EXPERIMENTS WITH INFRASONIC NOISE-REDUCING SPATIAL FILTERS

Michael A.H. Hedlin and Jon Berger

Scripps Institution of Oceanography; University of California, San Diego

Sponsored by Defense Threat Reduction Agency

Contract No. DTRA01-00-C-0085

ABSTRACT

As development of the International Monitoring System (IMS) infrasound network progresses, there remains much to learn about reducing noise due to atmospheric turbulence while preserving signals from distant sources. The spatial filter currently preferred for use at new IMS infrasound array sites consists of an array of low-impedance inlets connected by solid tubes to a microbarometer. Acoustic signals and noise enter the "rosette" pipe system via the inlets and are summed in manifolds or at the sensor. Acoustic energy that is incoherent at wavelengths less than the aperture of the filter is attenuated, and the ratio of coherent signal to incoherent noise is increased. We have tested two designs of rosette filters that span 18 and 70 meters to estimate the signal-to-noise ratio (SNR) gain as a function of wind speed and to look for artifacts of the filtering process. Empirical observations compare well with theoretical predictions. The 70-m filter provides noise reduction of up to 20 dB over a band from 0.02 Hz to 0.7 Hz. The 18-m filter does not suppress noise below ~ 0.2 Hz. The corner frequency of both spatial filters scales directly with wind speed. Resonance is observed in data from both filters but is most pronounced in data from the 70-m filter. Modeling of data from both filters clearly indicates that the reflections occur at all points inside the filters at which the impedance changes. Although a large impedance change occurs at the low-impedance inlets, the resonance that is first observed at 0.7 Hz in data from the 70-m filter, and at 3 Hz in data from the 18-m filters occurs between the primary and secondary summing manifolds. Experiments show that this resonance can be largely, or entirely, removed by installing impedance matching capillaries adjacent to the secondary summing manifolds in the pipes leading to the primary summing manifold. Adding capillaries at the inlets is less effective as those points are linked with high-frequency resonance at the upper limit, or beyond, the passband of interest to the monitoring community.

Rosette filters are tuned to vertically incident energy. Energy arriving at other incidence angles is not summed in phase. The problem is acute at high frequencies, at near-horizontal arrival angles, and scales directly with the aperture of the filter. Total cancellation of the horizontally propagating signals recorded via the 70-m rosette filter is predicted to occur at 5 Hz. Recordings of a large bolide that exploded west of the infrasound test bed in southern California on April 23, 2001, were made by co-located reference systems and the large and small rosette filters. The data validate the phase and amplitude response predicted by a theory that takes into account the resonance of energy inside the filters and the phase delays of the energy entering the filters.

This paper will report these results and our experiments with noise reducing barriers.

OBJECTIVE

Our objective is to build, model and test infrasonic noise reduction systems to assess the utility of the different devices as a function of frequency and wind speed. Our goal is to test systems that are being deployed at International Monitoring System (IMS) array sites and to test new devices (such as the new fiber optic sensor under development at the University of California San Diego [UCSD], Zumberge et al., 2002) and spatially compact filters (such as the wind barrier, a sensor buried at a shallow depth in a porous medium) in our search for systems that are more economical, require less space, or have a better response than currently preferred designs. We identify shortcomings of filters (e.g. resonance in large pipe filters) and search for ways to improve the filters.

RESEARCH ACCOMPLISHED

Preliminary evaluation of rosette filters

We have conducted tests of rosette infrasonic noise-reducing spatial filters (Alcoverro, 1998) at the Pinon Flat Observatory in southern California (Figure 1; Hedlin et al., 2002). Data from 18- and 70-m-aperture rosette filters (Figure 2) and a reference port have been used to gauge the reduction in atmospheric wind-generated noise levels provided by the filters and to examine the effect of these spatial filters on spatially coherent acoustic signals in the 0.02- to 10-Hz band. At wind speeds up to 5.5 m/s, the 18-m rosette filter reduces wind noise levels above 0.2 Hz by 15 to 20 dB. Under the same conditions, the 70-m rosette filter provides noise reduction of up to 15 to 20 dB between 0.02 and 0.7 Hz. Standing wave resonance inside the 70-m filter degrades the reception of acoustic signals above 0.7 Hz. The fundamental mode of the resonance, 15 dB above background, is centered at 2.65 Hz and the first odd harmonic is observed at 7.95 Hz in data from the large filter (Alcoverro and LePichon, 2002; Hedlin et al., 2002). Synthetics accurately reproduce the noise reduction and resonance observed in the 70-m filter at all wind speeds above 1.25 m/s (Figures 3 and 4). Resonance theory indicates that internal reflections, which give rise to the resonance observed in the passband, are occurring at the summing manifolds, and not at the inlets. Rosette filters are tuned to acoustic arrivals with infinite phase velocity. Attenuation of signals by the 70-m rosette filter at frequencies above 3.5 Hz arriving at grazing angles of less than 15° from the horizontal are predicted to range upward from 10 dB to total cancellation at 5 Hz (Figure 5). Theoretical predictions of the phase and amplitude response of 18- and 70-m rosette filters that take into account internal resonance and time delays between the inlets compare favorably with observations derived from a cross-spectral analysis of signals from the explosion of a large bolide (Figure 6).

Experiments with impedance-matching capillaries

We have conducted three experiments with impedance-matching capillaries to remove the problem with resonance in the rosette spatial filters (Hedlin and Alcoverro, 2002). In the first test, we sought confirmation that the reflections that give rise to the resonance peaks observed at 2.65 and 7.95 Hz in the data from the 70-m rosette filters are occurring at the secondary summing manifolds, and not at the inlets. We constructed three filters that consist of 8- to 27-m-long pipes. We fitted the open ends of the pipes with different capillaries to assess the utility of acoustic resistance for removing the resonance problem. The test reproduced the resonance peaks and confirmed that the reflections that give rise to the spectral peak at 2.65 Hz occur at the primary and secondary summing manifolds. The test, and subsequent modeling, also confirmed that the resonance peaks could be completely removed by installing capillaries at the inlets of these simplified filters. The appropriate acoustic resistance of each capillary is the characteristic impedance of the pipe that connects the inlet with the primary summing manifold. Modeling also confirms that the same capillaries will remove the resonance problem in the complete rosette filters. Installing eight capillaries adjacent to the secondary summing manifolds in the pipes leading to the primary manifold will be far more effective than installing the capillaries at the 144 inlets (Figure 7). Data collected from a filter in the infrasound array I57US that was modified with capillaries, with acoustic resistance equal to the characteristic impedance of the 27-m pipes connecting the primary and secondary summing manifolds, revealed that the main resonance peak at 2.65 Hz is completely removed, as predicted by theory, and the first sign of resonance, due to resonance in the pipes between the secondary summing manifolds and the inlets, is observed at 5 Hz (Figure 8). A separate test of capillaries in the 18-m rosette filters produced similar results. All filters in the IMS infrasound array I57US have been modified with capillaries as a result of this research. Modeling indicates that a modest improvement of the response of the 70-m rosette filter can be achieved by installing capillaries at the inlets, but this

is not recommended because of the plane wave response, mentioned in the previous section, that degrades the response of these filters above 3 Hz.

Tests of noise-reducing wind barriers

This section reports empirical observations of wind speed and infrasonic noise reduction inside a wind barrier. The barrier has been compared with "rosette" spatial filters and with a reference site that uses no noise reduction system. The barrier is investigated for use at IMS infrasound array sites where spatially extensive noise-reducing systems cannot be used because of a shortage of suitable land. Wind speed inside a 2-m-high 50% porous hexagonal barrier coated with a fine wire mesh is reduced from ambient levels by 90%. If the infrasound wind noise level reductions are all plotted versus the reduced frequency given by $f*L/v$, where L is the characteristic size of the array or barrier, f is the frequency and v is the wind speed, the reductions at different wind speeds are observed to collapse into a single curve for each wind-noise-reduction method. The reductions are minimal below a scale size of 0.3 to 1, depending on the device; then spatial averaging over the turbulence structure leads to increased reduction. Above the corner frequency, the fence reduces infrasonic noise by up to 20 to 25 dB (Figure 9). Below the corner frequency the barrier displays a small reduction of about 4 dB. The rosettes display no reduction below the corner frequency. One other advantage of the wind barrier over rosette spatial filters is that the signal recorded inside the barrier enters the microbarometer from free air and is not integrated, possibly out of phase, after propagation through a system of narrow pipes.

CONCLUSIONS AND RECOMMENDATIONS

Rosette filters

We have found that modeling theory, which takes into account reflection and attenuation of acoustic energy in the rosette filters and includes the response of the microbarometer, accurately reproduces recorded data. We have also determined that impedance matching capillaries, installed at the secondary summing manifolds, will remove the resonance problem. We have noted that the rosette filters are tuned to vertically incident acoustic waves and the reception of signals that arrive within 15° of the horizontal is limited. The plane wave response is most significant in the large, 70-m-aperture rosette filter.

We recommend that all rosette filters used at IMS infrasound arrays are modified as described in the earlier section.

Future research with rosette filters

The theory that accounts for internal resonance and external phase delays can be applied to any rosette filter design and therefore, in principle, can be used to search for better designs. This could be accomplished by defining optimization criteria (e.g. lack of resonance peaks in the band below 10 Hz; flat plane wave response in the same band) and systematically searching for designs that optimally satisfy these criteria. It remains to be determined if the combined theory can be used to correct the amplitude and phase of signals filtered through rosette filters.

Real rosette filters do not adhere perfectly to the specified designs shown in Figure 2. Most sites present obstacles that require some modifications to the placement of the inlets in the rosette clusters. Most sites are not perfectly horizontal but are tilted. An important question that we can now begin to address is what the rosette filters do to the overall performance of an infrasound array. What asymmetries in the placement of the inlets and what tilts at the different elements can exist before unacceptable bias will be introduced into the back-azimuth derived from processing data from all elements. If these imperfections in the locations of the inlets and in the tilts of the filters are known, this work might lead to a means to remove this bias.

Arrivals from naturally occurring infrasound sources such as bolides can be used as signals of opportunity to calibrate *in situ* the amplitude and phase response of the IMS space filters. The derived "calibration" curves can be used to help remove the system response from the recorded data. These calibration curves are a function of arrival angle (apparent phase slowness) as well as frequency so that a collection of events in various directions is required to obtain a complete set of empirically derived curves. Alternatively, one or two events can be used to validate a theory of the spatial and frequency dependence of the rosette filter response, as is done in Hedlin, Alcoverro and D'Spain (2002), so that theoretically derived calibration curves then can be applied. Changes in conditions at the

recording site can result in changes in the filter response. For example, variations in atmospheric temperature result in changes in sound speed that, in turn, cause a shift in the frequencies of the resonances and in the location of the spatial response null associated with phase delays. Likewise, a change in the number, location, and effective impedance of individual ports in a rosette filters will affect the resonance and spatial nulling characteristics. The impact of such changes on the filter response can be evaluated using the methods described in Hedlin, Alcoverro and D'Spain (2002).

Theoretical tests of capillaries are needed to determine the effect of one or more of the capillary plugs becoming partially or fully blocked by water, insects, etc., on the response of the individual filters and of the entire array. The long-term maintenance of these systems might involve periodic inspection and clearing of the capillary plugs.

Wind barriers

Comparison of the scaled reductions in wind noise produced by the rosettes and wind barrier with the reductions afforded by a spherical wind screen hold promise for significant wind-noise reduction with a smaller footprint device (Hedlin and Raspet, 2002). The rosettes only produce reductions if the scale size of the turbulence is smaller than the size of the rosette since such devices rely on the incoherence of the turbulence at each port. The wind barrier displayed large reductions only when the scale size of the turbulence is smaller than the height of the barrier. However, a small reduction of about 4 dB was realized when the scale size was larger than the barrier. This reduction may correspond to the large reductions realized by foam windscreens. In the spherical windscreens, these reductions occur since the pressure measured at the center is the area average of the pressures generated at the surface of the sphere. For large turbules, the pressure generated by an increase in wind speed is positive at the front of the sphere and negative at the back, and the average is less than the pressure measured at a bare sensor. This result holds promise that a properly designed windscreen on or near the ground surface may achieve significant reductions even for turbulence scales greater than the size of the screen.

ACKNOWLEDGEMENTS

Our research was conducted collaboratively with Rich Raspet (University of Mississippi), Benoit Alcoverro (DASE France), and Gerald D'Spain (UCSD). We would like to acknowledge pioneering work on the wind barrier by Ludwik Liszka (Swedish Institute of Space Physics). The design of the wind barrier and insights into how the barrier reduces infrasonic noise were provided by Doug Revelle (Los Alamos National Laboratory). We thank Hank Bass (University of Mississippi) for constructive comments on our research with the wind barrier. The authors are indebted to Chris Hayward (SMU) and Doug Christie (CTBTO) for suggesting that we experiment with capillaries. Frank Vernon, Jennifer Eakins and Glen Offield provided the real-time data link. Clint Coon provided field assistance. Funding was provided by the Defense Threat Reduction Agency under contract DTRA01-00-C-0085. Funding for the rosette filters used in this study was provided by the Defense Threat Reduction Agency, the Provisional Technical Secretariat (PTS) of the Comprehensive Nuclear-Test-Ban Treaty Organization in Vienna, and the US Army Space and Missile Defense Command (SMDC) University Research Initiative (URI).

REFERENCES

Alcoverro, B. (1998) Acoustic filters design and experimental results, Proceedings: Workshop on Infrasound, Commissariat à l'Energie Atomique, Bruyères-le-Châtel, France, July 21-24, 1998.

Alcoverro, B. and A. Le Pichon (2002) Design & optimization of a noise reducer system for infrasound measurements using elements with low acoustic impedance, submitted to *J. Acoust. Soc. Am*.

Hedlin, M.A.H., B. Alcoverro, and G. D'Spain (2002) Evaluation of rosette infrasonic noise-reducing spatial filters, manuscript in review with the *J. Acoust. Soc. Am*.

Hedlin, M.A.H. and B. Alcoverro (2002) The use of impedance matching capillaries for reducing resonance in rosette spatial filters, manuscript in preparation for the *J. Acoust. Soc. Am*.

Hedlin, M.A.H. and R. Raspet (2002) Evaluation of an infrasonic noise-reducing barrier, in preparation for *J. Acoust. Soc Am.*, submitted June 14, 2002.

Zumberge, M.A., J. Berger, M.A.H. Hedlin, R. Hilt, S. Nooner, and R. Widmer-Schnidrig (2002) An optical fiber infrasound sensor: a new lower limit on atmospheric pressure noise between 1 Hz and 10 Hz, in preparation for *J. Acoust. Soc Am*., submitted June 14, 2002.

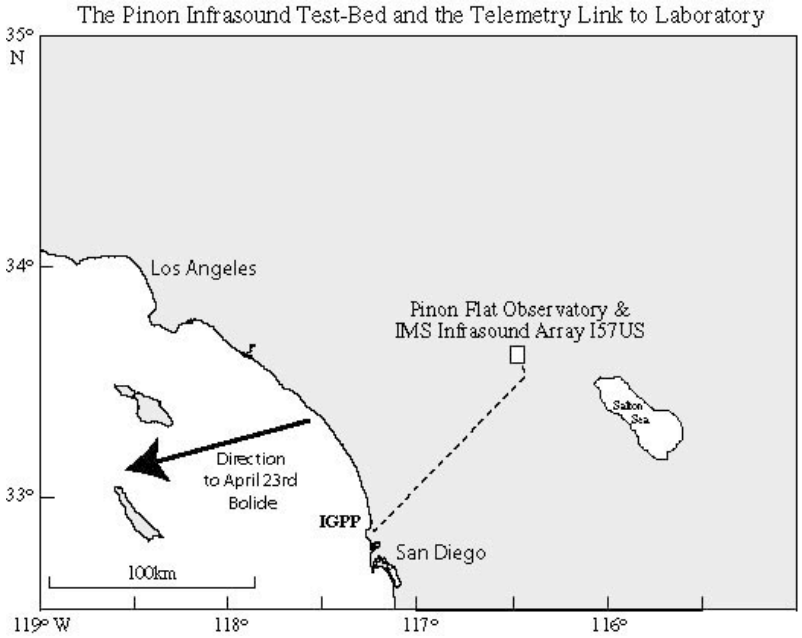

Figure 1. The IMS infrasound array, I57US, is located in the Anza Borrego desert at the Cecil H. and Ida M. Green Pinon Flat Observatory (PFO). The infrasound test-bed is located at PFO. The real-time radio-telemetry link to the laboratory (IGPP) is also shown. Signals from a large bolide that exploded to the SW of the observatory are used in this paper to calibrate the rosette filters.

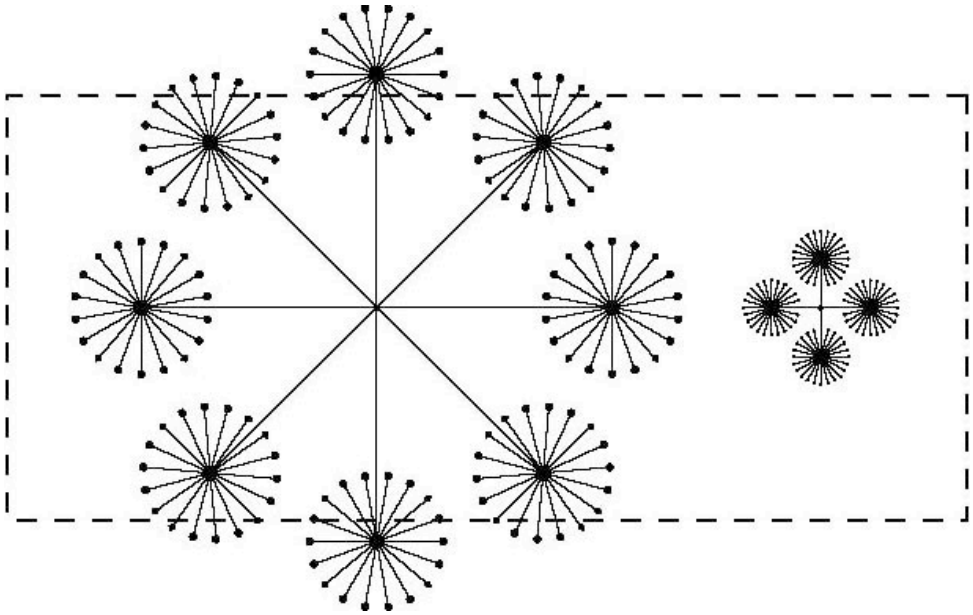

Figure 2: Two rosette filters considered in this paper are shown to scale with a National Football League playing surface. The 18-m filter comprises 92 low-impedance inlets in four rosettes. The 70-m filter comprises 144 inlets arranged in eight rosettes.

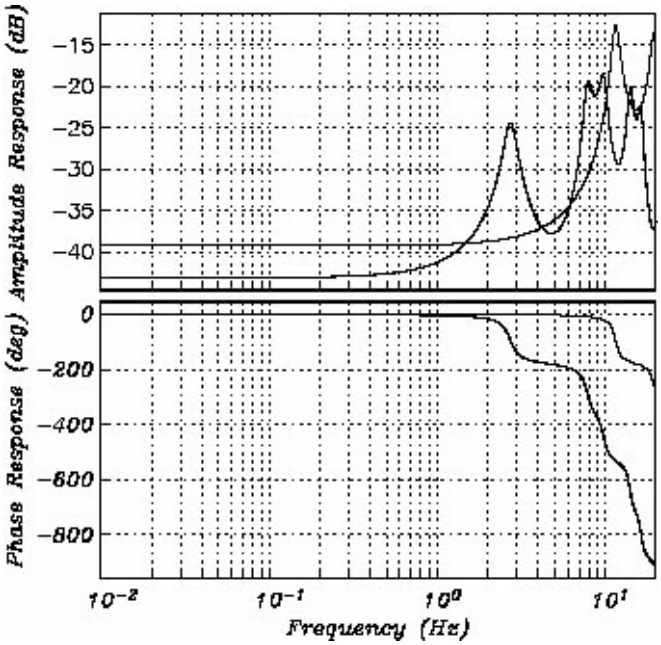

Figure 3: Predicted amplitude and phase response of the 18-m/92 rosette filter (light curve) and the 70-m/144 rosette filter (bold curve) for one inlet. The resonance peaks coincide with significant change in the phase response of the filter. The long-period response is given by -20 log10(N), where N is the number of inlets.

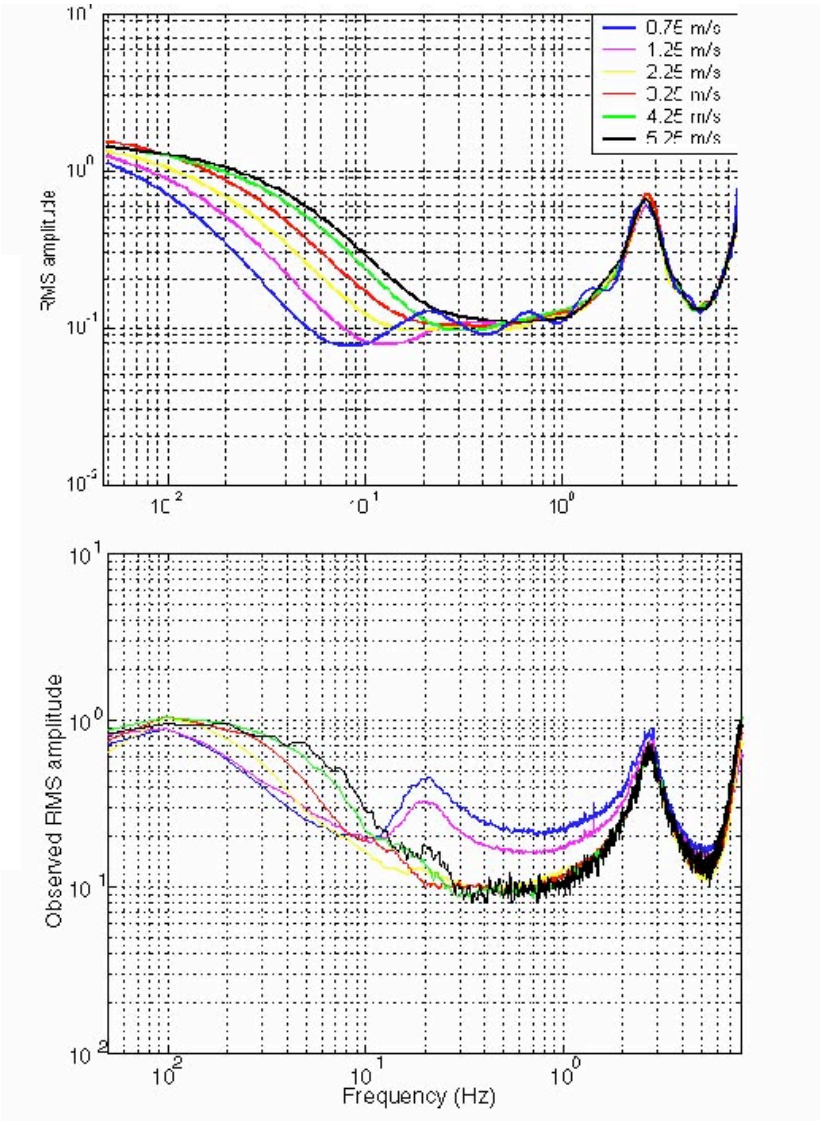

Figure 4: Simulated noise reduction of the 70-m/144-port rosette filter for various mean wind speeds is shown in the upper panel. Each curve represents the ratio between the noise spectrum observed at the reference port and the noise spectrum of the rosette system. The corner frequency of the 70-m rosette filter is predicted to increase with increasing wind speed. Observed noise reduction is shown in the lower panel.

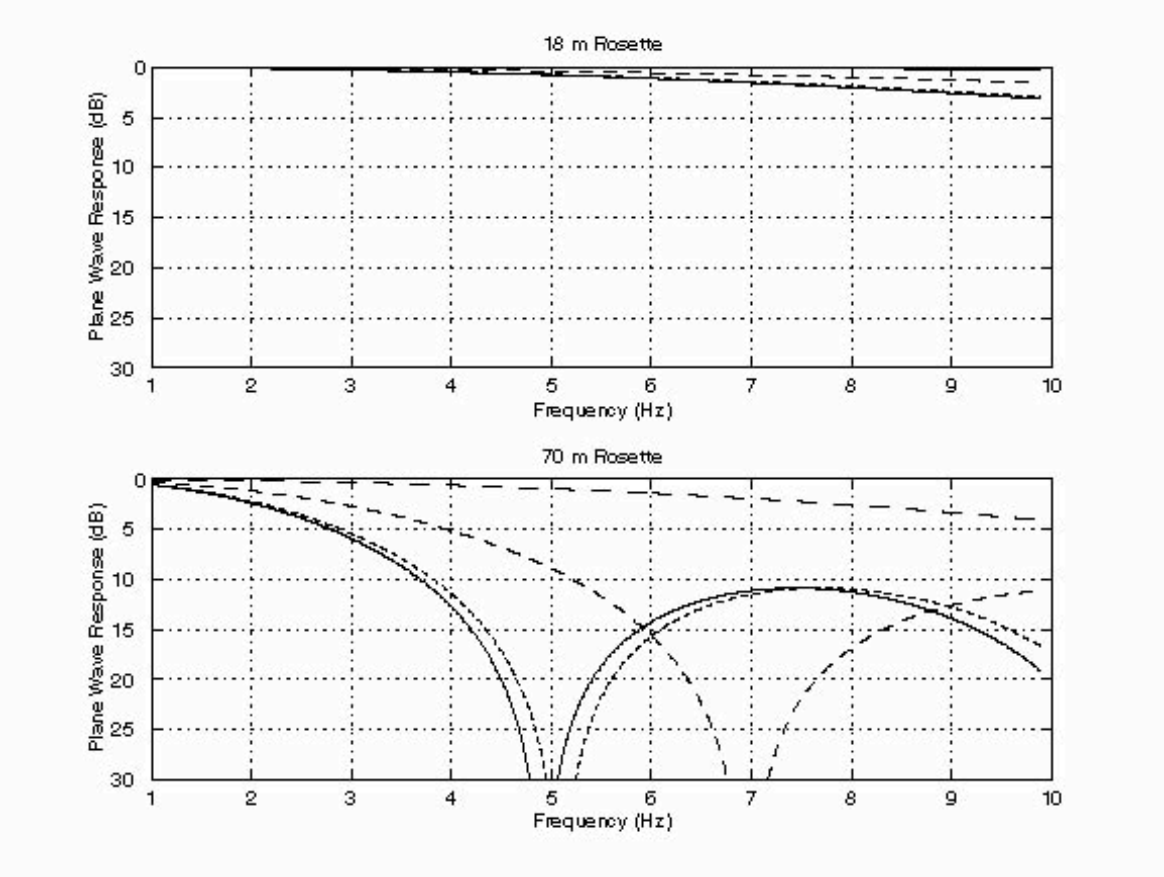

Figure 5: The rosette filter integrates pressure variations from the inlets simultaneously regardless of the angle of incidence of the arriving energy. The rosette filter is tuned to vertically incident signals. Attenuation of signals increases with increasing arrival angle from the horizontal and with increasing frequency. The attenuation is strongly dependent on the aperture of the filter. For example, in the upper and lower panels we show the plane wave response for the 18- and 70-m rosette filters respectively at four arrival angles. The solid curves in each panel represent an arrival with an arrival angle of 0° above the horizontal. The finely to coarsely dashed curves represent signals propagating across the two filters at 15, 45 and 75° above the horizontal. The elevation angles, θ_e, are calculated assuming a sound speed, c, of 347 m/s. The phase velocity, c_p, is given by c/cos (θ_e). The phase velocities corresponding to the arrival angles at the four arrival angles are 347, 359, 491 and 1341 m/s. In both panels, the response for a vertically incident signal is 0 dB at all frequencies.

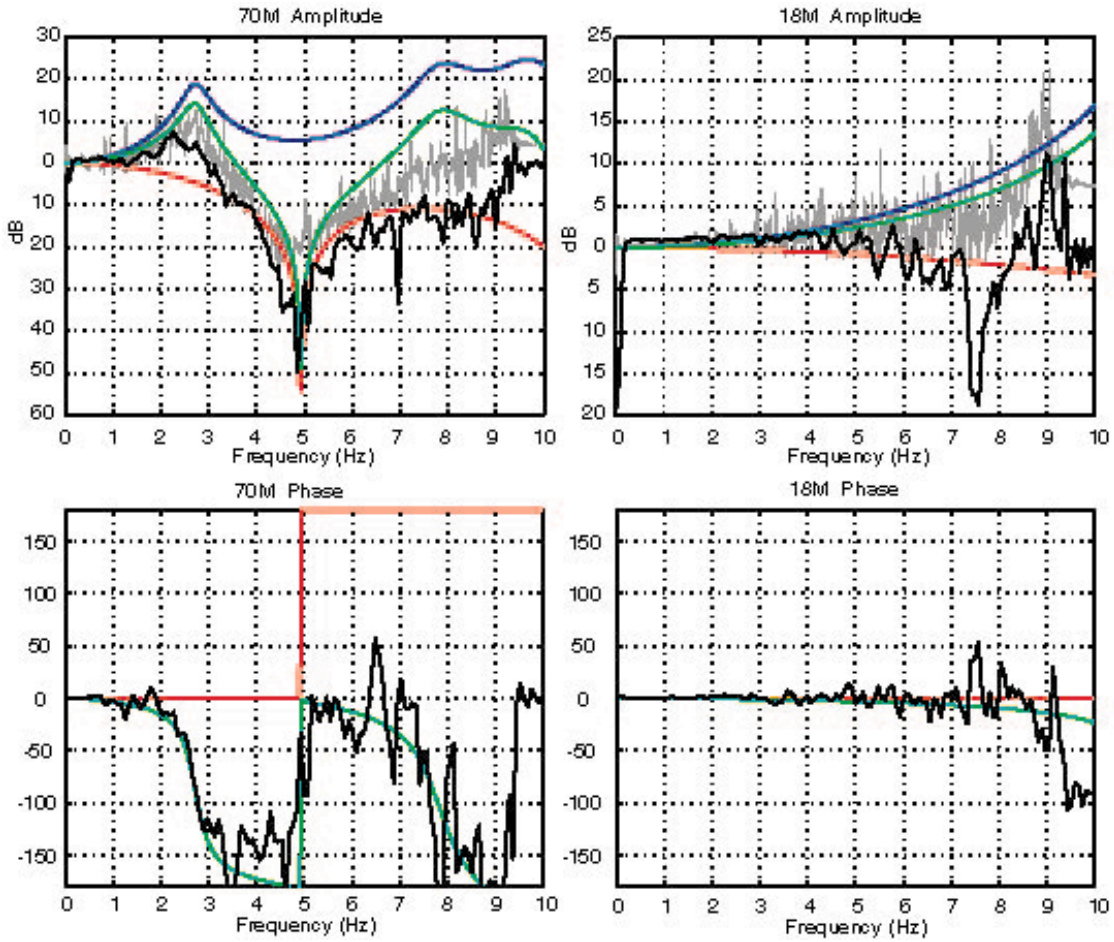

Figure 6: Amplitude and phase response of 18- and 70-m rosette filters are shown in this figure. The blue curves in all panels represent the response due to internal resonance inside the pipe systems. The red curves represent the plane wave response. The plane wave response of the filters, which is dependent on the phase velocity of the incoming energy, has been calculated at 330 m/s. This is the phase velocity of the energy from the April 23rd bolide as determined by processing data from the I57US array. The green curves represent the total response due to time delays between inlets and to resonance inside the filters. As shown in Figure 9, the 18-m filter attenuates the incident signal by less than 5 dB at all frequencies up to 10 Hz. The attenuation caused by the 70-m filter is strongly frequency dependent at this low phase velocity. A pronounced notch is predicted to exist at 5 Hz. Amplitude and phase from a phase-coherent cross-spectral analysis of data from the April 23rd bolide are shown in black. The theory accurately predicts the phase of the signal but under-predicts the amplitude at all frequencies. A spectral ratio of the filtered to unfiltered data (gray curves in the upper panels) closely match the theoretical predictions.

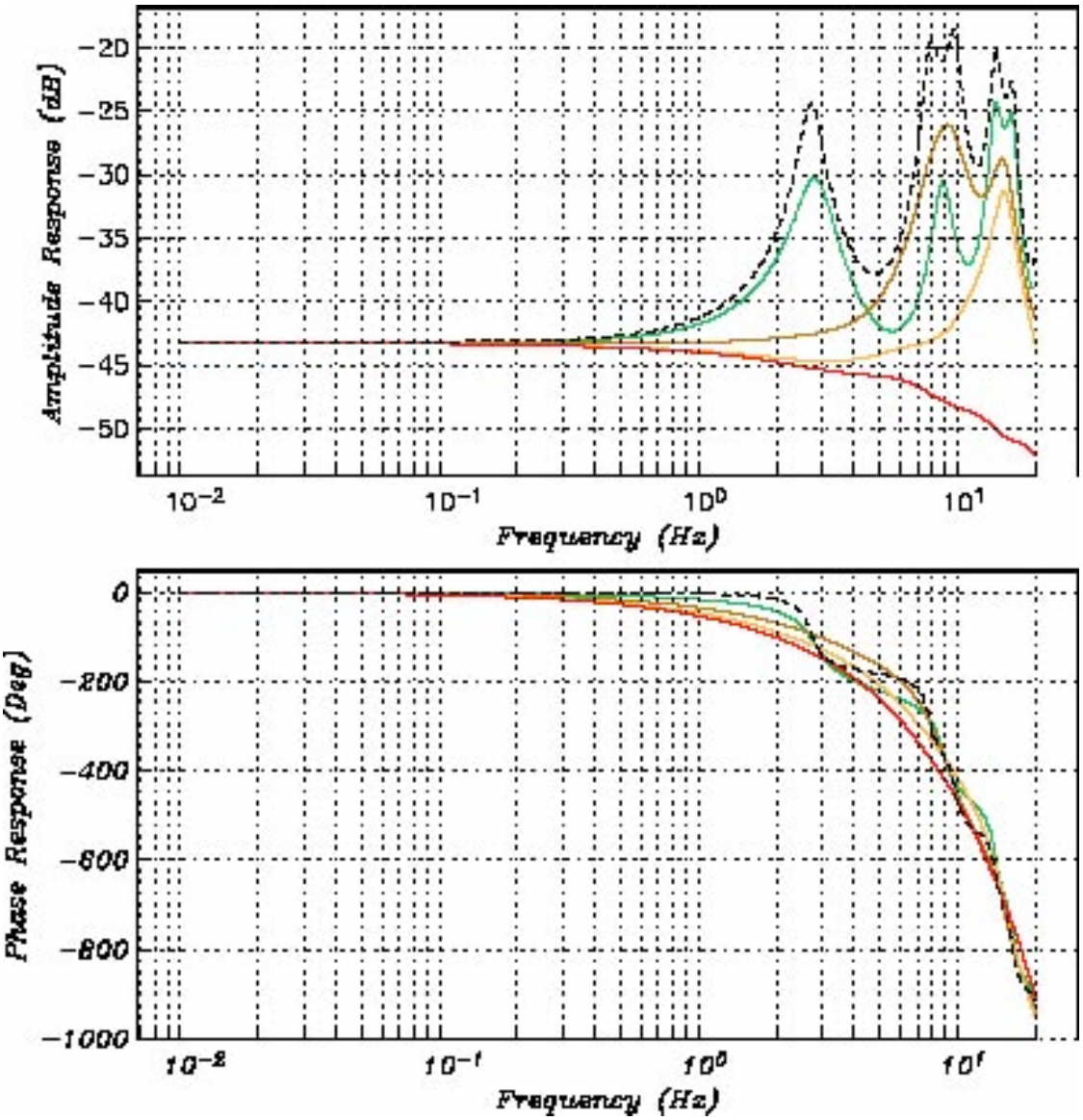

Figure 7: Simulations on the original and modified 70-m-aperture rosette filters are shown in this figure. The systems with capillaries at the inlets, secondary summing manifolds, both the inlets and the secondary summing manifolds, at the inlets and both summing manifolds are represented by the brown, green, gold and red curves. The unmodified system is represented by the dashed curves.

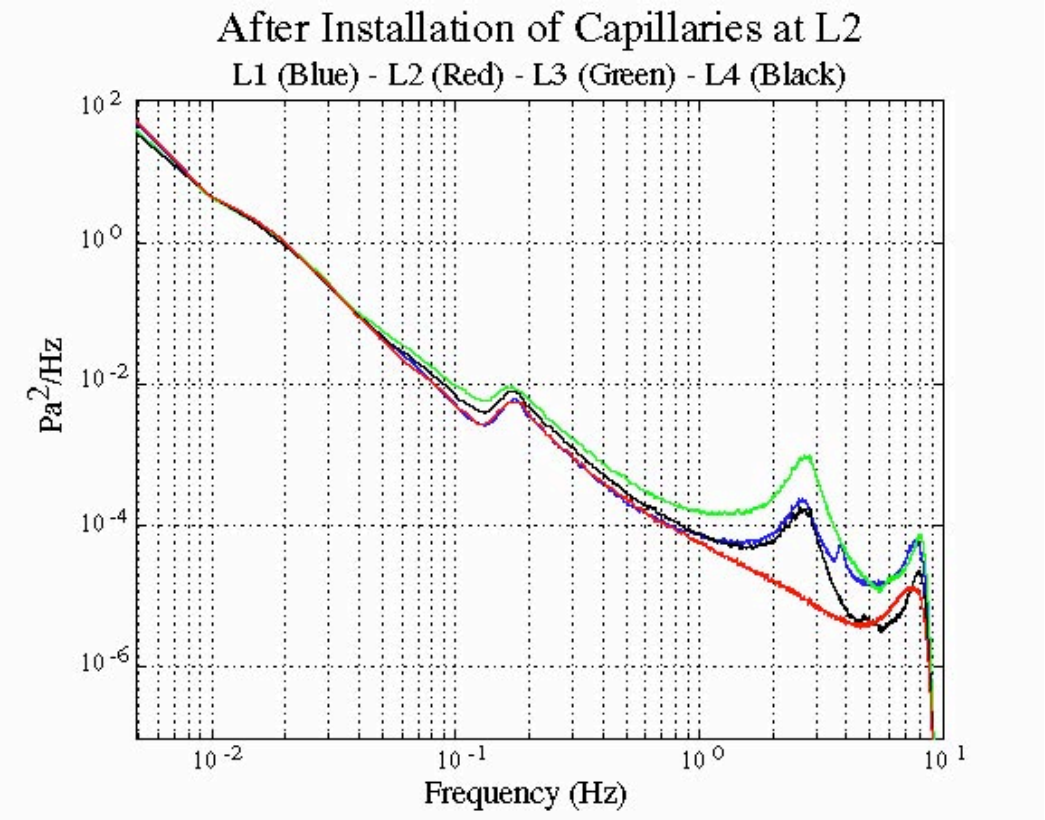

Figure 8: Spectral density estimates taken from data collected after the capillary plugs were installed at site "L2" (red curve). The capillaries have removed the resonance peak at 2.65 Hz.

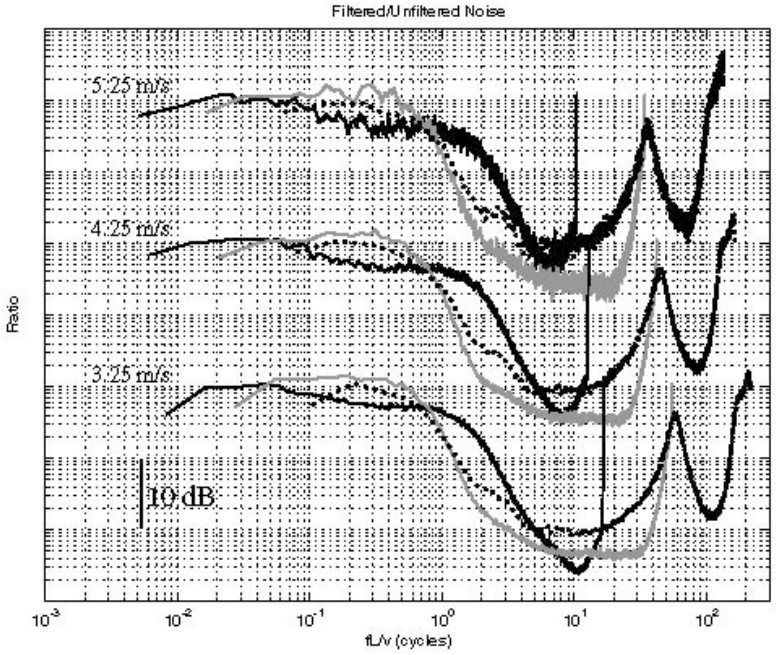

Figure 9. Wind-noise reduction versus scaled frequency at 3.25m/s, 4.25m/s, and 5.25m/s for the 70- rosette (bold dots), the 18-m rosette (bold gray) and the 5.5-m wind barrier (solid curves).